Complete and selective recovery of lithium from EV lithium-ion batteries: Modeling and optimization using oxalic acid as a leaching agent

Separation and Purification Technology 320 (2023) 124143

Contents lists available at ScienceDirect

Separation and Purification Technology

journal homepage: www.elsevier.com/locate/seppur

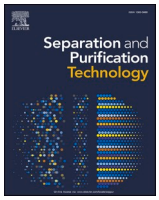

Complete and selective recovery of lithium from EV lithium-ion batteries: Modeling and optimization using oxalic acid as a leaching agent

Léa M.J. Rouquette *, Martina Petranikova, Nathália Vieceli

Department of Chemistry and Chemical Engineering, Industrial Materials Recycling and Nuclear Chemistry, Chalmers University of Technology, Kemivägen 4, SE-41296, Gothenburg, Sweden

ARTICLE INFO

Keywords:
Lithium recovery
Oxalic acid
Selective leaching
Recycling
Battery

ABSTRACT

The necessity of a feasible process for the recycling of lithium-ion batteries is nowadays evident due to the significant demand for raw materials for battery production, but also due to legislative requirements to achieve certain recycling efficiency with sufficient quality of the products. Special conditions to achieve high lithium recovery and its use in new batteries represent a challenge for a commercial hydrometallurgical approach. In this work, an early selective recovery of lithium using oxalic acid as a leaching agent is investigated. The different solubility of transition metals oxalates in comparison to lithium oxalate was the main driving force to achieve selective separation in the leaching step. Nickel, cobalt, and manganese oxalates are insoluble and remained in the solid residue, while lithium oxalate was dissolved in the solution. Using a design of experiments to optimize the operation, optimal parameters were identified as 60 °C, 60 min, 0.6 M oxalic acid, resulting in 98.8% leaching yield for lithium, while less than 0.5 % of cobalt and nickel, and 1.5% of manganese were leached. This can significantly improve the lithium recovery in the current recycling processes. Moreover, aluminum was completely dissolved, which is a phenomenon not reported previously. It would constitute an advantage to the subsequent recycling operations.

1. Introduction

The achievement of the climate goals has required an acceleration in the deployment of the so-called “clean energy” such as wind power or solar panel. Moreover, reaching net-zero emissions globally by 2050 will demand an even more dramatic increase in the implementation of clean energy technologies over the same timeframe [1]. These energy systems involve the use of robust energy storage technologies. Transport is one of the major contributors of green-houses gases (GHG), in fact, it was accounted for 37% of CO_2 emissions from end-use sectors in 2021 [2], which represents around 15% of global emissions of GHG. The main part of these emissions is caused by road transport and passenger travel accounting for 3/4 of the sector’s emissions [2]. As a result, in the last decade, the transport sector underwent a strong shift toward its electrification. To support and enhance this fast change, the European Union announced that by 2035, only zero-emission vehicles will be sold within its borders, giving a deadline to the end of gasoline, diesel, and hybrid vehicles [3]. These different incentives have driven the electric vehicle (EV) sales market to increase by 40% from 2019 to 2020 [1].

The lithium-ion battery was the technology of choice to develop 85.6% of the energy storage systems already in 2015 [2]. Lithium, cobalt, and nickel play a central role in giving batteries greater performance, longevity, and higher energy density. Looking at the developing trends in the lithium market, only between 2020 and 2021, the consumption of lithium showcased a radical increase of 33% [4]. Escalating demands have hence raised the question regarding the sustainability of lithium extraction. Today, most of the consumed lithium is extracted either from natural ore minerals or salt lakes coming essentially from Australia, South America, and China. Only 1% of the lithium reserves are found in Europe, thus, the reliance of Europe for lithium is total and lithium was added to the list of critical raw materials in 2020 by the European Commission [5].

To maximize the access to raw materials, metals are being recycled from secondary resources. It is estimated that 250 tons of ore are processed to produce 1 ton of lithium (lithium carbonate equivalent - LCE), while 256 EV batteries would be needed to achieve the same production. The Global Electric Vehicle Outlook 2022 reports that the recycling rate for lithium is lower than 1% [1,6] and the official End-of-life recycling input in the EU is 0% [6]. However, it is very hard to have updated data and official statistics around the recycling of lithium-ion batteries and an

* Corresponding author.
E-mail address: malea@chalmers.se (L.M.J. Rouquette).

https://doi.org/10.1016/j.seppur.2023.124143
Received 22 February 2023; Received in revised form 15 May 2023; Accepted 18 May 2023
Available online 27 May 2023

even more precise recovery rate of the element. For instance, some Chinese media report that 30 to 40% of battery materials are recycled [7]. In 2019, in pv magazine, Hans Eric Melin, director of Circular Energy Storage said, "We know from our data that about 100,000 tons of waste batteries were recycled last year, that's about 50% of what reached end-of-life" [8]. To secure the supply chain of batteries, the European Union is developing a new Regulation proposal stronger than the previous Directive 2006/ 66/EC controlling batteries' life, as it will oblige any member state to apply this legislative act in their country. The traceability of batteries will be a key element to promote their collection and recycling. Some specific recovery targets are also announced: 70% of the lithium from electric vehicle (EV) batteries is required to be recovered by 2030 and 6% of recycled lithium must be input into new batteries [9]. These high targets represent a challenge for the industrial stakeholders but also enforce the research and development around lithium recovery and purification technology.

Currently, there are two main families of recycling processes. Historically, pyrometallurgy is a well-settled process, capable of handling large volumes and inhomogeneous feed material, but this goes along with gas emission and high energy consumption. Moreover, the lithium is lost as it ends up in the slag after the treatment along with aluminum and manganese [10]. Research is ongoing for its recovery from the slag using hydrometallurgy, but a feasible process is not expected in the upcoming years. On the other hand, hydrometallurgy allows to achieve higher recovery rates and requires lower energy consumption, but it is a more complex and chemically intensive process. A traditional flowsheet starts with the dissolution of valuable metals from the black mass during an acidic leaching operation assisted with a reducing agent such as hydrogen peroxide, followed by separation steps where the metals can be selectively recovered one after the other using solvent extraction or precipitation. Finally, purification technologies are needed to obtain products that can be reintegrated into the battery production [11]. Some robust processes already exist but lithium is very little recovered and suffers losses all along the recycling process since its recovery is commonly addressed at the end of the recycling circuit [11,12].

In this work, the feasibility of an early selective and complete recovery of lithium by leaching with oxalic acid was investigated using a black mass sample from spent EV batteries (which was industrially produced using crushing and mechanical sorting). A design of experiments was used to define the best operating conditions, which were validated with a scale-up of the operation under optimal conditions. The objective was to optimize the acid consumption and to define the mechanism of the leaching process using oxalic acid.

Lithium was separated from the rest of the valuable elements, cobalt, nickel, and manganese as their respective oxalate without any addition of reductant. This selective lithium recovery with a reduction of impurities in the leachate is the main achievement of this study. Very high selectivity was targeted in this work as it is beneficial for many reasons, especially the simplification of the recycling process which would require fewer purification steps. Moreover, aluminum behavior was followed during the operation and its total dissolution was observed. This has the potential to significantly improve the process of impurities removal as aluminum is a difficult element to remove from the black mass using the traditional route with sodium hydroxide. In addition, oxalic acid is a very good candidate as it has a high potential for industrialization, is easily produced biologically or commercially, and is considered a more environmentally friendly alternative to inorganic acids [13].

2. Background on battery recycling using organic acids

In traditional hydrometallurgical processes, the black mass from spent lithium-ion batteries (after discharging, dismantling, crushing, and sorting) is dissolved in inorganic acids such as sulfuric acid, hydrochloric acid, and nitric acid, usually with the addition of a reducing agent such as hydrogen peroxide. Then the leached metals are selectively recovered and purified using different techniques such as solvent extraction, precipitation, or crystallization. The use of these inorganic acids is associated with various emissions (gas releases such as SO_3, Cl_2, or NOx depending on the acid used) and the formation of waste streams and wastewater [13].

Avoiding gaseous emissions, organic acids are usually considered more environmentally friendly than classical inorganic agents [13,14]. Various organic acids have been studied for the recycling of spent batteries, among them malic and citric acids were largely investigated. However, being weak acids (pKa1 = 3.4 for the malic acid and pKa1 = 2.79 for the citric acid), they were not strong enough to dissolve the oxides and required the addition of a reducing agent [14]. For instance, Yanan Tu et al. [15] studied the leaching of spent NCM cathode material (incinerated at 800 °C) using DL-malic acid and glucose as the reductant. The leaching yields reported were 90.1 % for nickel, 90.6 % for cobalt, 98.7 % for manganese, and 98.5 % for lithium (under the optimal conditions of 1 M DL-malic acid, 0.5 g/g glucose, 90℃ leaching temperature, and 25 g/L pulp density for 120 min). Borong Wu et al. [16] reported that 90% of cobalt and nearly 100% of lithium were recovered using citric acid assisted with hydrogen peroxide (1.25 M of citric acid, 1 vol% hydrogen peroxide, S/L = 20 g/L for 30 min at 90 °C with agitation at 300 rpm). Hongrui Ma [17] investigated the leaching of LCO cathode material with tartaric acid, attempting to separate lithium and cobalt during the operation. The optimal recovery of lithium (97%), associated with the smallest recovery of cobalt (2%), was obtained after a leaching time of 30 min, at 80 °C, a pulp density of 30 mL/g, and acid concentration at 0.6 M. However, the use of a reductant was needed to achieve this yield (3 vol% of hydrogen peroxide).

The oxalic acid is the strongest of the organic acids with dissociation in two steps (Pka1 = 1.23 and pKa2 = 4.19) but still weaker than other traditional inorganic acids (pKa1 = − 2.8 for the sulfuric acid). Nevertheless, it constitutes a good candidate as a leaching agent and reducing agent, and the mechanism of dissolution of metals by the oxalic acid is acid/complex based. First, it dissolves the metal oxides into the solution. Then, the ion oxalates, strong chelating agents, react with the metal ions forming metal oxalate complexes. The complexation reaction of oxalic acid for a simple oxalate can be described by equations (1) and (2) below.

$$n\left[HC_2O_4^-\right] + M^{n+} \rightarrow M[HC_2O_4]_n \quad (1)$$

$$n\left[C_2O_4^{2-}\right] + 2M^{n+} \rightarrow M_2[C_2O_4]_n \quad (2)$$

Lithium reacts with oxalate ion to form a simple oxalate, while copper, cobalt, manganese, and nickel are reported to form simple and complex oxalates, it is however more predictable to find simple oxalates for these metals [18]. Aluminum on the other hand is reported to form only complex oxalate compounds which are soluble in aqueous media, thus, consequent dissolution is expected.

Metals as simple oxalates are known to have low solubility, so they are expected to precipitate during the leaching process. This precipitation capacity of certain oxalates enables selective separation of the metals. Indeed, manganese, nickel, and cobalt oxalate were expected to remain in the solid phase while lithium should be dissolved, as it can be anticipated from the solubilities data in Table 1. Aluminum is reported to be dissolvable by oxalic acid in different studies in large proportions [19,20], however, aluminum oxalate is reported insoluble in aqueous media. Thus, special attention will be given to aluminum in this work

Table 1
Solubility and K_{sp} of oxalate compounds [21].

	$Li_2C_2O_4$	CuC_2O_4	MnC_2O_4	CoC_2O_4	NiC_2O_4
Solubility (g/L) at 18 °C	6.6	–	–	0.035	0.003
K_{sp}	–	$4.4.10^{-10}$	$1.70.10^{-7}$	$5.7.10^{-8}$	$4.2.10^{-10}$

since this fact was never applied to remove aluminum from lithium-ion batteries.

Some authors have already investigated oxalic acid as a leaching agent as reported in [22–27]. Table 2 presents the conditions applied in the different studies and the optimal recovery yield for each element. However, the behavior of copper and aluminum are not reported. Therefore, no yield data was reported in Table 2 for those last two elements. Chrul-Kyoung L. et al [22] compared sulfuric and oxalic acid leaching of $LiCoO_2$ (LCO) powder. More than 95% of the cobalt and lithium were leached using sulfuric acid (1 M sulfuric acid, at 80 °C for 90 min and a S/L of 50 g/L) but at least 10 vol% of hydrogen peroxide was needed to achieve this efficiency. Indeed, it was reported that only 65% of lithium and 40 % of cobalt could be extracted without the reductant. On the other hand, with 3 M oxalic acid, at 80 °C for 90 min and a S/L of 50 g/L, all the lithium was dissolved and less than 1% of cobalt was found in the leachate, while the remaining cobalt was in the solid phase as insoluble CoC_2O_4 [22]. The non-use of reductant consists of a real advantage for the leaching with oxalic acid. In another study, Keping Qiu et al [28] used LCO spent batteries from mobile phones, which they dismantled to treat only the cathode material on which they applied a vacuum pyrolysis (600 °C for 30 min) to separate the aluminum foil from lithium cobalt oxide particles. From this feed stream, 98 % of the lithium was extracted using 1 M oxalic acid with 15 vol% of hydrogen peroxide, and the best leaching conditions were reported to be 80 °C, for 120 min with a S/L of 50 g/L. In this work, aluminum is mentioned as an impurity in the leachate solution, but its leaching yield is not given [28]. In Bingyu Shen et al. [23] two different feed materials were tested, one standard LCO powder from Sigma Aldrich and a LCO powder obtained after the crushing of batteries from electronic devices. It was reported that the standard LCO had a better reactivity with oxalic acid than black mass.

In the different works [23,28], the main dissolution reactions were reported as seen in Equations (3) and (4):

$$4H_2C_2O_4 + 2LiCoO_2 \rightarrow Li_2C_2O_4 + 2CoC_2O_{4\,solid} + 4H_2O + 2CO_{2\,gas} \quad (3)$$

$$7H_2C_2O_4 + 2LiCoO_2 \rightarrow 2LiHC_2O_4 + 2CoC_2O_{4\,solid} + 4H_2O + 2CO_{2\,gas} \quad (4)$$

They also characterized how the oxalic acid excess can be used [23] as observed in equation (5–6-7). In this work, aluminum extraction is reported to happen in the case of oxalic acid excess, as seen in equation 7.

$$H_2C_2O_4 + Li_2C_2O_4 \rightarrow 2\,LiHC_2O_4 \quad (5)$$

$$H_2C_2O_4 + CoC_2O_{4\,solid} \rightarrow 2Co(HC_2O_4)_{2\,liquid} \quad (6)$$

$$3\,H_2C_2O_4 + Al \rightarrow Al(HC_2O_4)_3 + 3/2\,H_{2\,gas} \quad (7)$$

Equation (6) describes the transfer from the solid phase to the liquid phase when some oxalates are still available to react with the simple cobalt oxalate. Equation 7 proposes the formation of simple aluminum oxalate, which is insoluble in water, its behavior during the leaching is not further investigated in the work.

Therefore, the feasibility of using oxalic acid as a leaching agent for LCO is not a question, as high-efficiency rates are reported [22,23,25,26,28]. Other authors proposed to investigate the leaching feasibility of $LiNi_xMn_yCo_zO_2$ (NMC) cathode material instead. Renjie Chen et al. [29] showed that the leaching behavior with NMC cathode material slightly deferred from LCO material. The authors observed the presence of NMC in the leaching residue even after more than 2 h of operation and the leaching yield of lithium was limited to 81%. They indicated that the morphology and size of the aggregate NMC oxalate formed during the process increase with the leaching time, thereby covering some remaining NMC oxides, and preventing the reaction. Moreover, they identified more chances to find manganese oxalate in the leachate solution as it has a higher solubility than cobalt and nickel oxalate but less than 1.5% of the NMC was found in the leachate [29]. Ka Ming et al. [27] also investigated NMC leaching with oxalic acid and in their work, the co-dissolution of manganese was demonstrated. Indeed, for the starting leaching parameters tested (oxalic acid concentration = 1 M, S/L = 10 g/L, 95 °C for 12 h) 95.4% of lithium was dissolved along with 24% of manganese. Increasing the acid concentration led to an increase in the manganese recovery, and the same trend was observed when increasing the temperature. Unfortunately, the effect of time on the leaching behavior was not studied and very long dissolution times were applied (12 h). To selectively recover lithium, the authors precipitated manganese as manganese oxide using sodium hydroxide [27]. Gerold et al. investigated the leaching of NMC cathode material with oxalic acid after pyrolysis at 500 °C, the leaching parameters studied were a temperature of 25 and 40 °C, a time between 1 and 4 h at S/L of 100 g/L and 30% excess of oxalic acid. They showed that the leaching of lithium with oxalic acid is hardly affected by adding 5 vol% of hydrogen peroxide, which is supporting the decision to avoid reducing agents in the operation. It was also demonstrated that reducing temperature and increasing time was beneficial for the selectivity of the operation since less nickel and cobalt were dissolved [13].

In the different studies previously done, summarized in Table 2, the parameters influencing the leaching operation were identified as: reaction time, temperature, acid concentration, and solid-to-liquid (S/L) ratio, as well as the optimal parameters allowing the best recovery rate.

Table 2
Summary of conditions for lithium extraction using oxalic acid (OA) as leaching agent reported in the literature (only the best conditions are reported; optimal parameters for the leaching).

	Preparation of the feed material	[OA] (M)	S/L (g/L)	Temp (°C)	Time (min)	Stirring (rpm)	Leaching yield (%)				Ref.
							Li	Co	Ni	Mn	
LCO	LCO powder from cathode and anode after a series of crushing, magnetic separation from LiBs −18mesh)	3	50	80	90	300	99	0.4	–	–	[22]
LCO	- Dismantling and mechanical separation to recover the cathode electrode Vacuum pyrolysis (600 °C for 30 min) to separate Al foil from the active material, $LiCoO_2$ powder was used for leaching	1 15 vol% H_2O_2	50	80	120	300	98	–	–	–	[28]
LCO	Discharged, crushed by shear crusher, and sieved (size < 1.43 mm)	1	15	95	150	400	98	< 3	–	–	[23]
LCO	Commercial LCO material 99.8 % purity from Sigma Aldrich	0.46	15	100	5/6h	600	98	1	–	–	[25]
LCO	Commercial LCO material 99.8 % purity from Sigma Aldrich	0.23 0.46 M H_2O_2	15	70	100	600					[26]
NMC	- Dismantling and manual separation of the anode and cathode, then treatment with DMC to remove electrolyte residues Cathode foil treated with NMP to separate active material from the Al foil Pyrolysis of the active material powder (700 °C)	0.6	20	70	120	–	81	< 1.5	< 1.5	< 1.5	[29]
NMC	Commercial NMC (111, 532, 811) from Zhengyuan Material Co.	1	10	95	12 h	–	96	< 0.5	< 0.5	22	[27]

This important data was used to define the relevant range of parameters included in the design of experiments in this study, as it will be developed in Section 3.3. Bingyu Shen et al. [23] identified the process as chemically controlled, for this reason, the oxalic acid concentration will be investigated in this study along with the time and temperature. Leaving aside the S/L ratios which will be fixed at 50 g/L as it has shown good results and it is a good process value. An oxalic acid concentration of around 1 M seems to be a prerequisite. In this study, the aim is to work with milder conditions, therefore, minimizing the acid consumption is of concern. For this reason, the highest concentration tested was 0.9 M and the lowest 0.3 M. It was expected that at a lower concentration, the selectivity of the operation towards the other transition metals would be higher. The same logic was applied when choosing the temperature range and assuming that lower operating temperatures would be better for the industrialization of the process, thus, the temperature tested was from 35 to 65 °C. Finally, when choosing the time range, the goal was to be able to observe the behavior of the metals at the very beginning and very end of the leaching reaction.

3. Materials and method

3.1. Sample preparation: Industrial black mass from spent LiBs

The black mass used in this study was obtained from the dismantling of 150 kg EV spent lithium-ion batteries provided by Volvo Cars AB (Sweden). The battery packs were discharged by Volvo Cars AB and then dismantled down to the cell level by Stena Recycling AB in Sweden. The chemistry of the battery cells was NMC 111. The cells (120 kg) were then processed through three steps comprising crushing, mechanical sieving, and magnetic separation by Akkuser Oy (Finland) to get three main output fractions. The processing temperature stayed below 50 °C. No thermal treatment was performed on this black mass, which provides the opportunity to develop a lithium recovery process without the need of thermal processing, saving thus the energy and need for off gas treatment. The fine fraction obtained represents 58.5% of the initial weight and is composed of the active materials from the cathode and anode along with the current foils and separator. It was further sieved under 500 μm in the Industrial Materials Recycling group at Chalmers University of Technology (Sweden) to obtain a very homogeneous powder concentrated with the active material and further remove the current collector foils. The sieving of 70 g black mass was performed with a sieve shaker (Retsch) for 5 min at an amplitude of 1.2 mm in interval mode and a sieve aperture of 500 μm. These sieving operating parameters were chosen based on the recommendation from Retsch, to obtain reproducible sieving process [30]. The fraction under 500 μm was used in this work and the sampling was performed using the coning and quartering technique to divide an initial sample into halves until the desired sample weight was achieved. This procedure helps to reduce the uncertainty associated with grab sampling from a container [31]. The elemental composition of the fraction used in the tests was determined using aqua regia (HCl/HNO_3: 3/1 v/v - Merk Millipore hydrochloric acid 37% w/w and Merk Millipore Nitric acid 65% w/w) at 80 °C for 4 h to digest the solid samples. The obtained slurry was then left to cool down overnight, then filtrated (filter VWR 516–0811 – 11 μm particle size retention) and diluted in HNO_3 0.5 M (Merk Suprapure Nitric acid 69% w/w). The metal content was analyzed using inductively coupled plasma optic emission spectroscopy (ICP-OES, Thermo Fisher Scientific, Model iCAP™ 6000 Series).

3.2. Leaching experiments

Oxalic acid leaching experiments were performed in 20 mL glass vials with caps and magnetic stirrers were used for agitation (300 rpm). The oxalic acid was prepared by dissolving solid oxalic acid dihydrate (Sigma Aldrich, ≥99%) in Milli-Q water. Black mass samples weighing about 250 mg were used in each test, which were obtained through the quartering method, the solid to liquid ratio was not investigated and was fixed at 50 g/L. The leaching temperature effect was also investigated and for this, the solutions (oxalic acid) were heated, and the solid samples were only introduced in the vials when the defined temperature was reached. After adding the solid samples, the leaching time started to be recorded. After the leaching, the samples were immediately filtered (Syringe filter PTFE - Restek – particle size retention of 0.45 μm) to separate the solid residue from the liquid phase containing the dissolved metals. Directly, the leachate was diluted in HNO_3 0.5 M (Merk Suprapure Nitric acid 69% w/w), and the metal content of each sample was analyzed using ICP-OES. The leaching yield (η_i) can be calculated according to Equation (8).

$$\eta_i = \frac{C_i \times V}{m_0 \times \omega_i} \times 100 \tag{8}$$

where C_i is the concentration of the element i in the leachate (ppm), V is the volume of solution (L), m_0 is the weight of the sample (mg) and w_i is the weight percentage of the element i in the sample (%).

A scale-up of the experiments was realized with a double-enveloped glass reactor of 100 mL equipped with a hot water bath. The solid sample was introduced once the temperature of the oxalic acid solution reached 60 °C and was stabilized. This experiment was performed in triplicate. Samples (0.5 mL) were taken after 1, 3, 5, 15, 30, 60, 90, and 105 min and immediately filtered and diluted for ICP–OES analysis using the same procedure previously described to avoid any precipitation that could occur in the meantime. The pH of the solution was followed during the operation using a pH electrode (Metrohm 6.0258.600) connected to the Tiamo software to record the data. When the test was completed, the solid residue was collected after filtration and dried for 24 h in an oven (50 °C) for further material characterization. X-ray powder diffraction (XRPD, Siemens D5000 diffractometer) was used to characterize the initial solid samples and the solid residue after leaching (Cu K_α radiation, 10°-80° 2θ range, 15 rpm rotation speed, generator settings of 40 mA and 40 kV). The EVA software and the JCPDS database were used for analytical interpretation. FT-IR (Perkin Elmer Spectrum Two UATR) was used to analyze the powder over the range of 450 to 4000 cm^{-1} with a resolution of 2 cm^{-1} and 16 scans, to put in evidence the carboxyl groups from the oxalate in the residue.

3.3. Experimental plan: Factorial design of experiments

The leaching optimization was achieved through a factorial design of experiments, response surface methodology, and contour plots that assisted in the visual interpretation of the modeled responses. The effect of each factor is defined to be the change in response produced by a change in the level factor [32]. Each factor (X) comprised two levels (2^3 factorial design) and the process response (Y) was defined as the leaching yield of each metal (%). To apply this method, the factors were fixed beforehand, and the test order was randomized. The use of this methodology allowed the optimization of the experimental efforts, assessing the main parameters influencing the operation and modeling the process using a reduced number of tests.

The factors and respective levels used in this study can be observed in Table 3. The design factors are oxalic acid concentration, leaching time, and temperature. They were chosen based on the range of conditions

Table 3
Factors and respective levels considered in the factorial design of experiments.

Factors	Levels		
	Low	Center	High
	(-1)	(0)	(+1)
Oxalic acid concentration (M) (x_1)	0.3	0.6	0.9
Leaching time (min) (x_2)	15	60	105
Leaching temperature (°C) (x_3)	35	50	65

from the literature review previously presented at the end of section 2. When using such an approach, it was prioritized to set a representative working range of conditions, as the model obtained is only valid within the experimental limits. The S/L ratio was fixed 50 g/L to have sufficient dispersion of the slurry and efficient mixing.

The design matrix is presented in Table 4 following a cubic face-centered design, with axial points performed (2 k axial points) at a distance of $\alpha = 1$ from the central point to allow to estimate second terms and curvature. At the central level, the design was replicated four times to estimate the experimental error.

The coefficients of a linear second-order regression model representing the process response were fitted using the linear least squares method (second-order regression models with two- and three-way interactions), which was solved using Excel's regression analysis tool. Only statistically significant variables were included in the models (p-value less than 0.05) and the significance of the models were assessed using Analysis of Variance (ANOVA). The existence of pure curvature was evaluated by hypothesis testing and the variance of the response accounted by the models was assessed by the coefficient of determination (R^2).

4. Results and discussions

4.1. Black mass characterization

The elemental composition of each fraction obtained after sieving can be seen in Table 5. The coarse fraction (over 500 μm) represents 31 wt% of the total sample weight, containing 8.5% of aluminum and 19% copper. On the other hand, the fine fraction presented a much smaller content of aluminum and copper. The mass balance for the sieving operation demonstrates that 80% of the elements present in the active material (lithium, cobalt, nickel, and manganese) are found in the fine fraction, while only 38% and 22% of the total amount of copper and aluminum were in the fine fraction. Based on the XRD patterns (Fig. 1), the black mass was composed of NMC 111 particles, graphite, copper, and aluminum, which is validated by the elemental composition of the fine fraction under 500 μm.

4.2. Factorial design of experiments and regression models

The experimental conditions tested in the factorial design of experiments and the correspondent responses as leching efficiency for different metals are presented in Table 6. The fitted regression models

Table 4
Design matrix with the standard test sequence (S) and random test sequence (R).

Test Order		Coded variables			Real variables		
R	S	x1	x2	x3	Acid concentration (M)	Time (min)	Temp (°C)
12	1	−1	−1	−1	0.3	15	35
11	2	1	−1	−1	0.9	15	35
3	3	−1	1	−1	0.3	105	35
6	4	1	1	−1	0.9	105	35
8	5	−1	−1	1	0.3	15	65
14	6	1	−1	1	0.9	15	65
4	7	−1	1	1	0.3	105	65
13	8	1	1	1	0.9	105	65
17	9	0	0	0	0.6	60	50
10	10	0	0	0	0.6	60	50
1	11	0	0	0	0.6	60	50
2	12	0	0	0	0.6	60	50
5	13	−1	0	0	0.3	60	50
18	14	1	0	0	0.9	60	50
15	15	0	−1	0	0.6	15	50
7	16	0	1	0	0.6	105	50
9	17	0	0	−1	0.6	60	35
16	18	0	0	1	0.6	60	65

Table 5
Elemental composition (wt%) of different fractions from the black mass (*indicate the fractions used in the following experiments). Averages and standard deviation for triplicates.

Fraction / Element	Co	Ni	Mn	Li	Cu	Al	Fe	Total wt%
BlackMass wt%	10.5 ± 0.3	8.2 ± 0.2	7.5 ± 0.1	3.4 ± 0.1	7.8 ± 0.1	3.5 ± <0.1	0.2 ± 0.1	100
BM + 500 μm wt%	5.3 ± 0.2	4.6 ± 0.1	4.3 ± 0.1	1.8 ± 0.1	19.0 ± 2.0	8.5 ± 0.9	0.1 ± 0.1	31
BM −500 μm wt% *	10.8 ± 0.4	8.6 ± 0.3	8.0 ± 0.3	3.3 ± 0.1	4.3 ± 0.3	1.1 ± 0.1	0.1 ± 0.1	69

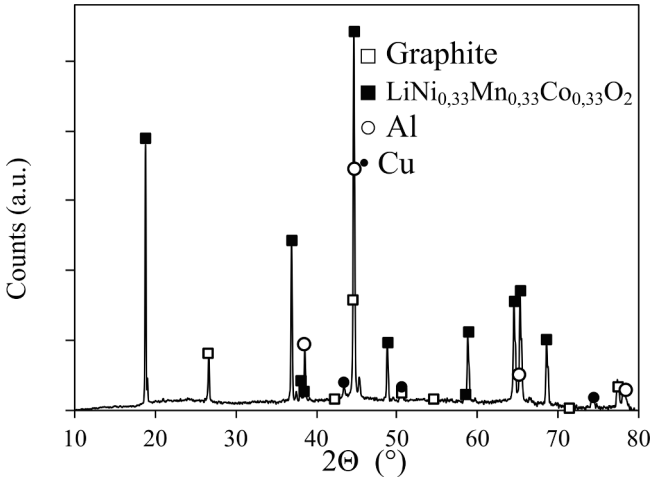

Fig. 1. XRD pattern for the fine fraction of the Black mass (under 500 μm); Graphite PDF 04–013-0293, $LiNi_{0.33}Mn_{0.33}Co_{0.33}O_2$ PDF 04–013-4379, Al PDF 01–071-4624, Cu PDF 04–009-2090.

for each metal and the coefficients of determination (R^2) are found in Table 7 (Equations 9 – 14). A sum-up of the significant parameters obtained for the regression model of each element is given in Supplementary Table S2. It is important to highlight that the models are valid within the range set in the experimental design and that only statistically significant terms are represented in each model (p-value less than 0.05). Tests 9 to 12 correspond to the replicates in the central level of design, which allow estimating the pure error, enabling the calculation of the lack of fit once the residuals are calculated. No experimental error could be determined for aluminum given its complete dissolution (leaching yield of 100%) in all the replicates in the central point.

The results for the analysis of the variance of the fitted model for lithium extraction are presented in Table 8. The significance of the regression model can be evaluated based on the F-value. Moreover, a Lack of Fit test was used to assess the model adequacy, but the value is slightly below the significant level of 0.0441. In this case, the variance of the residual error is higher than the estimated variance for the experimental error. This is not surprising considering the very small variation observed in the central point, therefore the experimental error is very low. The ANOVA results for other metals are presented in Supplementary Table S1.

The plot representing the observed response vs. the predicted response by the fitted model for lithium extraction is presented in Fig. 2 and demonstrates the goodness-of-fit of the model. The higher the coefficient of determination, R^2, the better the model fits the experimental data. Here, the R^2 is very high (99%), which indicates that the fitted model can describe well the variability in the data. The standardized effects of the evaluated variables were plotted using Excel software and

Table 6
Experimental design and correspondent responses expressed as leaching efficiency of different metals.

Tests (Std Order)	Coded variables			Real variables			Responses (Y) - Leaching yield (%)					
	x1	x2	x3	OA concentration (M)	Time (min)	Temp (°C)	Li	Al	Mn	Co	Ni	Cu
1	−1	−1	−1	0.3	15	35	39.6	41.7	5.1	1.0	3.0	4.0
2	1	−1	−1	0.9	15	35	43.2	42.2	6.3	1.0	3.0	2.9
3	−1	1	−1	0.3	105	35	71.1	90.4	4.0	1.1	2.5	5.4
4	1	1	−1	0.9	105	35	87.2	90.7	4.2	0.5	0.5	0.4
5	−1	−1	1	0.3	15	65	77.6	78.7	4.6	2.2	3.9	5.2
6	1	−1	1	0.9	15	65	91.1	93.0	4.9	0.5	0.4	1.0
7	−1	1	1	0.3	105	65	80.9	100.0	3.8	1.6	1.4	4.2
8	1	1	1	0.9	105	65	96.1	100.0	5.5	0.5	0.0	4.6
9	0	0	0	0.6	60	50	91.8	100.0	2.4	0.4	0.2	0.9
10	0	0	0	0.6	60	50	91.7	100.0	2.3	0.5	0.5	1.0
11	0	0	0	0.6	60	50	93.2	100.0	2.3	0.4	0.3	1.0
12	0	0	0	0.6	60	50	91.1	100.0	2.5	0.4	0.3	0.8
13	−1	0	0	0.3	60	50	76.3	75.6	4.4	1.9	3.5	7.3
14	1	0	0	0.9	60	50	95.6	100.0	3.9	0.5	0.3	0.6
15	0	−1	0	0.6	15	50	74.9	58.7	4.4	0.7	1.2	0.5
16	0	1	0	0.6	105	50	97.9	95.6	2.2	0.4	0.0	2.4
17	0	0	−1	0.6	60	35	74.9	70.7	4.3	0.5	0.8	0.4
18	0	0	1	0.6	60	65	96.6	100.0	2.7	0.5	0.0	3.4

Table 7
Regression models for leaching yield of each element with their respective R^2.

Equations	R^2	
$Li(\%) = 92.09 + 6.76x_1 + 10.68x_2 + 12.61x_3 - 8.40x_2x_3 - 6.33x_1^2 - 5.85x_2^2 - 6.50x_3^2$	0.99	(9)
$Al(\%) = 94.43 + 16.24x_2 + 13.58x_3 - 8.60x_2x_3$	0.92	(10)
$Mn(\%) = 2.64 - 0.55x_2 + 1.22x_1^2$	0.88	(11)
$Cu(\%) = 1.32 - 1.66x_1 + 2.28x_1^2$	0.85	(12)
$Co(\%) = 0.48 - 0.48x_1 - 0.29x_1x_3 + 0.16x_1x_2x_3 + 0.63x_1^2$	0.96	(13)
$Ni(\%) = 0.40 - 1.01x_1 - 0.70x_2 - 0.41x_3 - 0.37x_1x_3 + 0.52x_1x_2x_3 + 1.41x_1^2$	0.96	(14)

are represented as horizontal bars in the Pareto chart shown in Fig. 3 (a). The red dashed line indicates the significance level (p-value less than 0.05). The standardized effects of highly significant variables are located further to the right of the dashed line. Time and temperature are the variables with the main significant effect on lithium dissolution. No three-way interaction ($x_1x_2x_3$) or neither second-order acid concentration term (x_1x_2 and x_1x_3) were included in the reduced regression model Moreover, the normal probability plot in Fig. 3(b) is close to a straight line (R^2 = 98%), indicating that the residual distribution is approximately normal. Fig. 3(c) shows that the residual seems to be generally random, confirming the independence of the errors and the absence of correlation. No real pattern can be observed in Fig. 3(d), which shows that the residuals are structureless and unrelated to the response. Thus, the residuals are randomly distributed, and the modeling errors are normally and independently distributed. A similar analysis for every metal studied is presented in Supplementary Figure S1-S6.

The general observation we can make from the analysis of Table 6 is that the leaching yield for lithium and aluminum is very high (almost completely leached in certain conditions), while it is very low for the rest of the transition metals. Contour plots will be used to visualize better the leaching behavior of lithium and select the parameters allowing better dissolution.

4.3. Response surfaces and optimization

The response surfaces and contour plots for each element were plotted using Equations 9 – 14, and this method helps to highlight the relations existing between the different variables of the operation. The contours plots display a two-dimensional view of the response surface where all points that have the same response are connected to produce contour lines of constant responses. In a surface plot. the response surface is viewed as a three-dimensional surface.

The surface plots of lithium leaching yield are shown in Fig. 4, including yields between 50 and 100%. It is important to stress that its dissolution is influenced by all the factors investigated in this study. The oxalic acid concentration, time, and temperature have a positive effect on lithium dissolution. At the low level of each parameter, the yield is

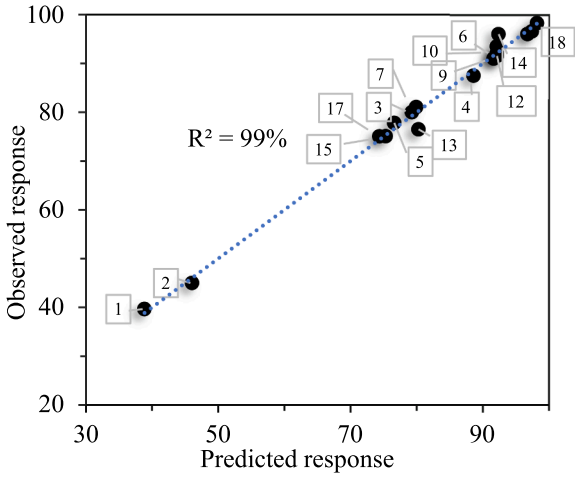

Fig. 2. Plot representing the observed response vs. the predicted response by the fitted model for lithium extraction for each test number.

Table 8
Results for the analysis of variance of the fitted model for lithium extraction.

ELEMENT	SOURCE	DEGREES OF FREEDOM	SUM OF SQUARE (SS)	MEAN SQUARE (MS)	F-VALUE	p-VALUE
Lithium	Total	17	4922.4	289.6	–	–
	Regression	10	4889.1	488.9	102.8	0.000001
	Residual	7	33.3	4.8	–	–
	Lack of Fit	4	31.0	7.7	10.0	0.0441
	Pure error	3	2.3	0.8	–	–

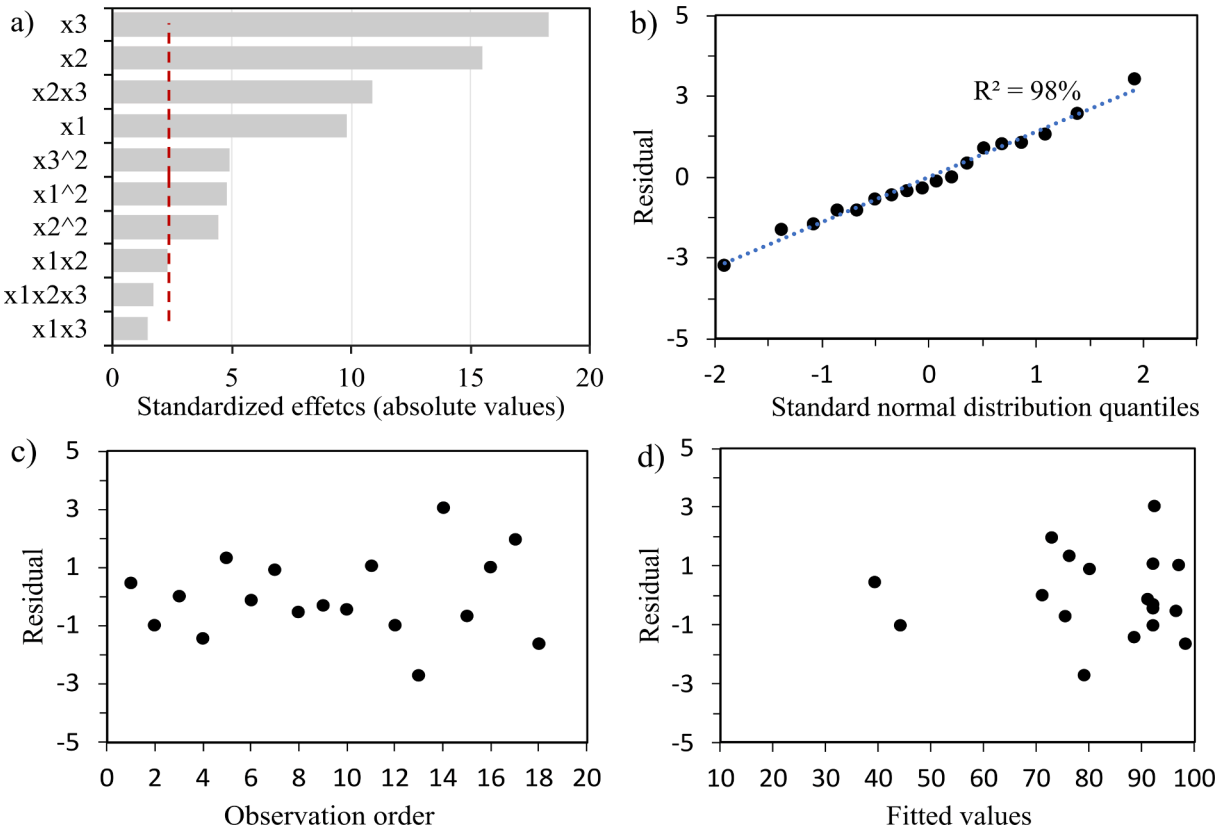

Fig. 3. Pareto chart of the standardized effects of the factors (x_1: acid concentration, x_2: time, and x_3: temperature) for the regression model of Lithium (a) and Analysis of residuals: standard normal distribution of the residuals (b), residual versus observation order (c), residuals versus fitted values (d), and Response predicted by the model versus experimentally observed response (e).

around 50% only and it reaches more than 90% at the central level of the design. Considering the goal of reaching the complete dissolution of lithium with milder conditions, it is already possible to target a different set of parameters that will allow an extraction over 95%: oxalic acid concentration of 0.6 M at 55 °C for 60 min or oxalic acid concentration of 0.6 M at 40 °C for 105 min. Under 0.45 M of oxalic acid, less than 90% of the lithium is extracted.

The aluminum dissolution is not influenced by the oxalic acid concentration as seen in Equation (3); one contour plot is relevant to observe the factors influencing the extraction as seen in Fig. 5. It is shown that the dissolution increases with the temperature and time from 50% of extraction in the smaller range of time and temperature (15 min and 35 °C) to over 100% of extraction when the temperature goes over 60 °C and long leaching time. Complete extraction of aluminum was not expected and not reported by previous authors, who reported aluminum as a simple impurity without focusing on its leaching behavior. To validate the absence of aluminum in the leaching residue, an elemental analysis of the leaching residue was performed, and this is discussed in section 3.4. The total extraction of the aluminum does not represent a problem in the rest of the recycling process since aluminum is normally removed before the separation of the transition metals, thus having a leaching residue free of aluminum is convenient. However, the purification of the leaching solution will be investigated in future work, using for example precipitation or solvent extraction. Moreover, we consider that the efficiency of the mechanical pre-treatment can be improved, and the current foils could be further removed from the black mass stream.

The behavior of the other elements was also tracked (Fig. 5), as predicted by Ka Ming et al. [27] manganese is the element the more extracted by oxalic acid due to the solubility of manganese oxalate. In this study, at the central point, 2.4% of manganese was leached, which is lower than the dissolution previously observed by Ka Ming et al. [27] (around 20%). That can be explained by the dissolution time applied in their work, 12 h. Indeed, the time has a positive effect on the dissolution of manganese as seen in the regression model, Equation 11. Thus, if the reaction proceeds for a long time, the transition metals have more chance to be found in the leachate if there is some oxalate available to react with. Nevertheless, the leachability of manganese is not considered problematic since it reached low yields, and manganese is not as valuable as the other transition metals. Moreover, it can be precipitated as $Mn(OH)_2$ when removing the aluminum from the leachate solution using sodium hydroxide. Equation 11 shows that the dissolution process of manganese is not influenced by the temperature. At smaller concentrations, we can see that the final extraction decreased with time from about 4% to 0%. This highlights the 2 steps mechanism of the leaching, with first the dissolution of the manganese as manganese oxalate that then precipitates. On the other hand, higher concentration enhances higher leaching yield, up to 3.5%. Indeed, the insoluble oxalate can react with the oxalate excess present in the solution forming soluble complexes.

When looking at the other transition metals (Fig. 6), nickel, and cobalt dissolution remains lower than 1% with a decrease when the temperature is increased. Moreover, the time is influencing the dissolution, the longer the reaction is left running, the more the elements can be found as complex oxalate in the leachate. This correlates with the observation done on manganese dissolution.

Finally, the copper dissolution is influenced only by the oxalic acid concentration and a dissolution of around 1% was achieved using 0.6 M of oxalic acid. After the investigation of all the elements, the best set of parameters allowing the highest lithium yield, but the lowest dissolution

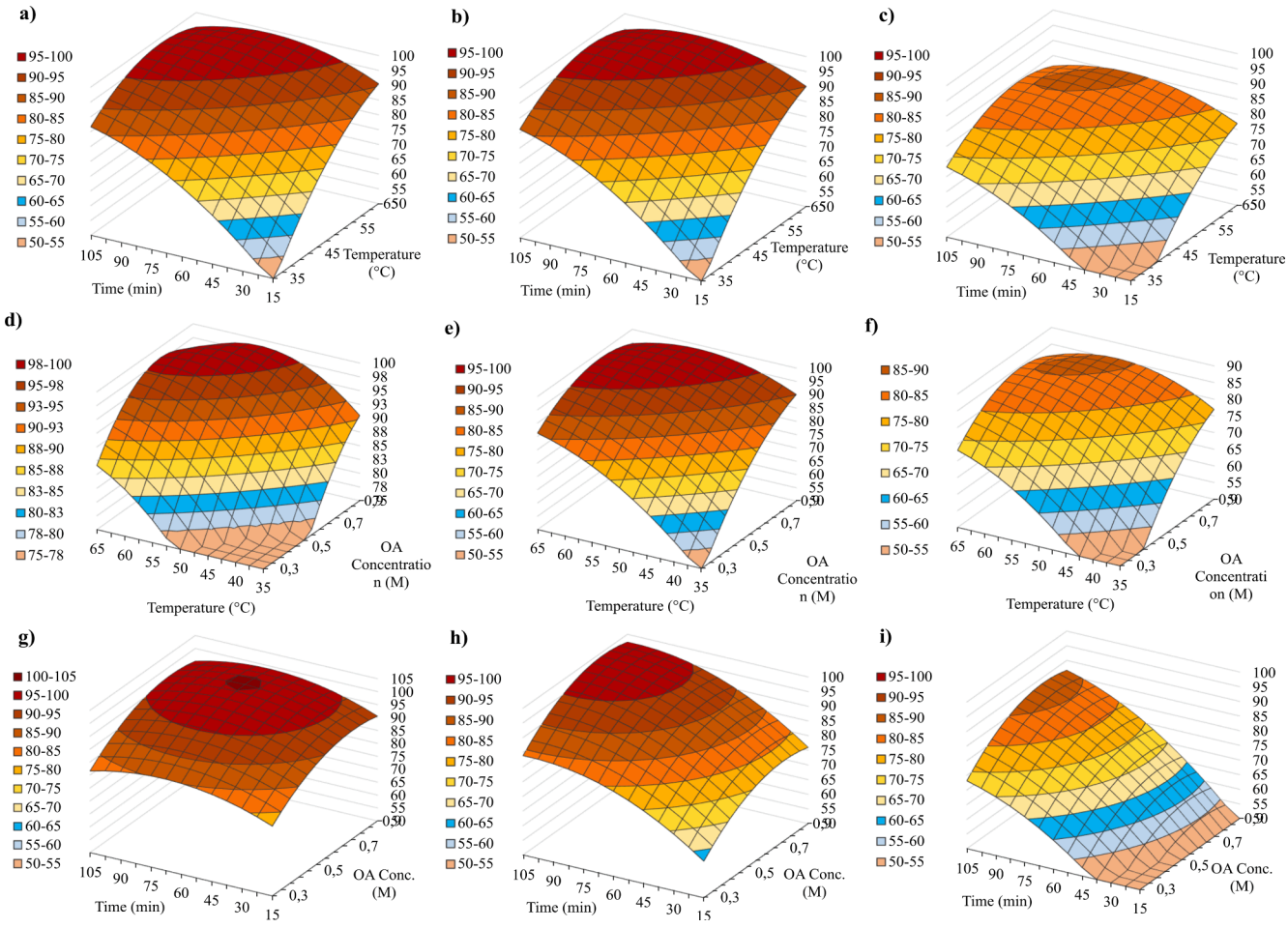

Fig. 4. Lithium contours plots a) 0.9 M of oxalic acid, b) 0.6 M, c) 0.3 M, d) 105 min, e) 60 min, f) 15 min, g) 65 °C, h) 50 °C, and i) 35 °C.

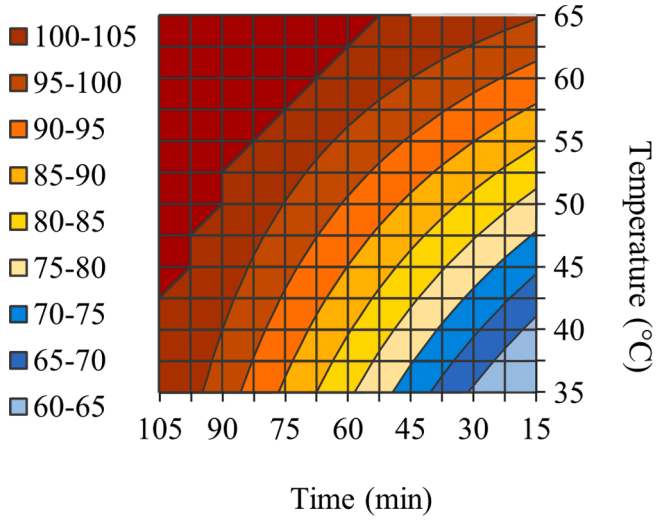

Fig. 5. Aluminum leaching yield contour plots for oxalic acid concentration set at 0.3 – 0.6 – 0.9 M.

of the transition metals was identified and corresponds as: temperature = 60 °C, S/L = 50 g/L, oxalic acid concentration 0.6 M. These conditions were used in the upscaled experiments discussed in the following section to validate the regression models, but also to produce leaching residue to further investigate and confirm the leaching mechanism.

4.4. Upscaling the operation at optimal conditions

4.4.1. Validation of the fitted models

The leaching yields observed in the upscaled experiments under optimal conditions (temperature = 60 °C, S/L = 50 g/L, oxalic acid concentration 0.6 M) can be seen in Fig. 7. It is possible to observe that in 30 min all the aluminum is leached, which validates the observation made in the design of experiments and suggests the formation of aluminum oxalate complexes during the leaching operation.

The leaching kinetics for lithium is having a two-rate speed – in the first 15 min, the dissolution is very fast and then it slows down, which can be explained by the pKa_1 that is reached after 8 min. 60 min were required to fully leach lithium. On the other hand, the dissolution of manganese, cobalt, and nickel decreases with time as they precipitate as oxalates. Copper dissolution slightly increased after 60 min, but although this behavior was not predicted by the model, which indicated independence from time, the final copper dissolution was very low (4.1%). The pH reaches a plateau after 60 min, increasing from 0.8 at the beginning of the reaction to 1.9. It is also important to highlight the average concentration of lithium in the leachate is 1.7 g/L ± 0.1 against 0.60 g/L ± 0.01 g/L of aluminum (while 9 ppm of cobalt was detected and 37 ppm of copper).

A comparison of the predicted leaching yields calculated using Equations 9–14 with the obtained experimental values is presented in Table 9. It was confirmed that the fitted models are quite accurate when determining the leaching yield of lithium, aluminum, and copper, but had a higher deviation for nickel, cobalt, and manganese as very low extraction is observed for these metals. Moreover, it was observed that the selectivity of the operation is higher than predicted by the models,

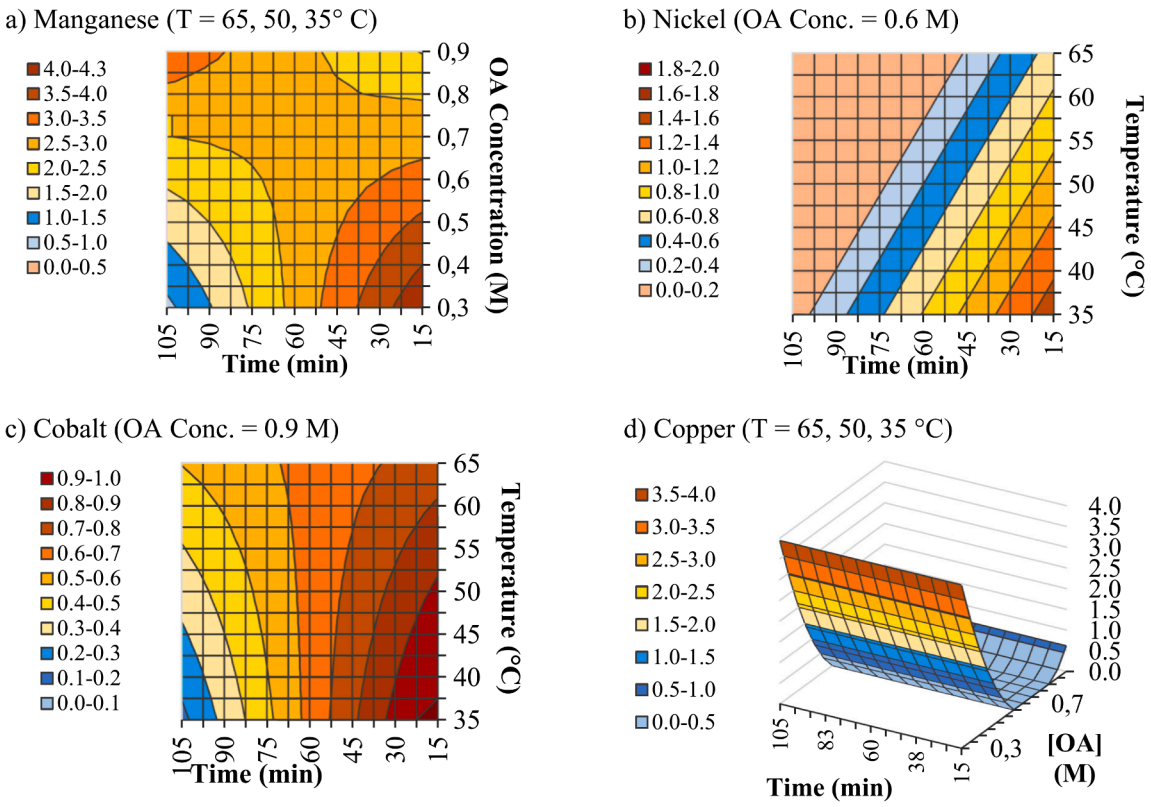

Fig. 6. Contour plots representing leaching yield and modelled responses for manganese (a), nickel (b), cobalt (c), and copper (d).

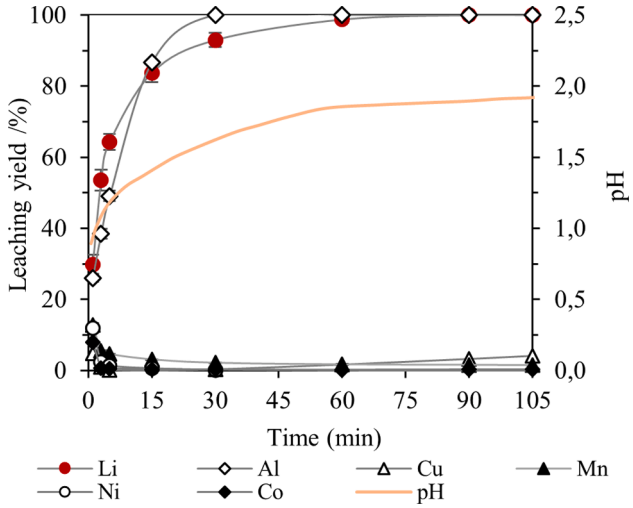

Fig. 7. Leaching yields and pH evolution during the upscaled leaching experiment. Leaching conditions: temperature = 60 °C, S/L = 50 g/L, oxalic acid concentration 0.6 M.

which is very promising for the future development of the process.

The leachate purification will be explored more deeply in future work. Different techniques can be considered such as solvent extraction or precipitation, for example, aluminum can be precipitated using sodium hydroxide. Then, lithium can be recovered as lithium carbonate after precipitation with sodium carbonate, as performed in the work done by Ka Ming et al [27].

4.4.2. *Leaching residue characterization*

The leaching residue was recovered after vacuum filtration and dried. The visual color of the residue turned from dark black after sampling to a lighter grey color, and an increase in weight was observed. Indeed, the initial sample weight inserted in the leaching reactor was 3 g, and the residue recovered gained about 17% ± 3% weight. The elemental composition of the leaching residue is shown in Table 10 and the results validate the leaching yields calculated. No trace of aluminum was detected, confirming its total dissolution, while only 0.4 % of residual lithium was detected. This constitutes an important finding of this work, since other authors did not observe a leaching of aluminum as high as shown in this work. There is a decrease in the elemental composition of other elements in the residue when compared to the

Table 9
Leaching yield predicted (P) and experimental (E) with the STD of the experimental data (STD E) comparison after 60 min, and the standard deviation (STD P/E) between the two values as well as the RSD P/E.

Element	Co	Ni	Mn	Li	Cu	Al
Yield P. (%)	0.48	0.18	2.64	97.7	1.32	100
Yield E. (%)	0.16	0.00	1.67	98.8	1.68	100
STD E. (%)	0.04	0.07	0.12	1.0	0.12	0
STD P/E. (%)	0.16	0.09	0.48	0.5	0.18	0
RSD P/E. (%)	100	–	29	1	11	–

Table 10
Elemental analysis of the leaching residue in %wt (* indicates the input material).

Element / Fraction	Co	Ni	Mn	Li	Cu	Al	Fe
BM −500 µm wt% *	10.8 ± 0.4	8.6 ± 0.3	8.0 ± 0.3	3.3 ± 0.1	4.3 ± 0.3	1.1 ± 0.1	0.1 ± 0.1
Leaching residue wt %	8.0 ± 0.1	7.1 ± 0.1	6.1 ± 0.1	0.4 ± 0.0	2.9 ± 0.1	0.0 ± 0.0	/

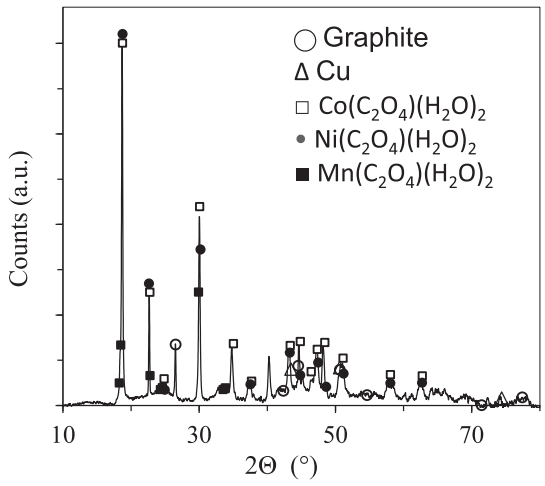

Fig. 8. Leaching residue XRD pattern; Graphite PDF 04–013-0292, Cu PDF 04–009-2090, $Co(C_2O_4)(H_2O)_2$ PDF 04–016-6937, $Ni(C_2O_4)(H_2O)_2$ PDF 04–016-6938, $Mn(C_2O_4)(H_2O)_2$ PDF 01–086-6854.

initial sample, but this gap is explained by the gain of mass of the residue due to the oxalate formation. The XRD pattern (Fig. 8) put in evidence the nickel, cobalt, and manganese oxalates in the residue. Copper and graphite remain in the residue as they have not reacted with the oxalic acid. However, there is no evidence of remaining cathode-active material in the form of NMC 111 in the residue as observed by Renjie Chen et al. [29]. This difference can be explained by the analytical method applied. Assuming all the lithium remaining in the residue is some unreacted NMC cathode material and considering the very small amount of lithium (0.4%), the detection of NMC material by XRD is compromised under its limit of detection. The FT-IR spectra in Fig. 9 reveals five main peaks. The first peak at 3373.5 cm^{-1} is attributed to the residual hydration of the oxalates compound (O–H stretching vibration). The peak at 1622 cm^{-1} is assigned to the asymmetric O-C-O of the carboxyl group, while the peaks at 1359.5 and 1314.5 cm^{-1} are associated with the symmetric of the same carboxyl function. Therefore, the FT-IR measurement correlates with the XRD analysis showing the precipitation of nickel, cobalt, and manganese oxalate, and these findings were also verified in the work of Qui K. et al [28].

More studies will be performed on this leaching residue to recover the transition metals from graphite and copper.

A proposition of the overall leaching reaction can be given after the characterization of the leaching residue, as seen in Equations (15) and (16):

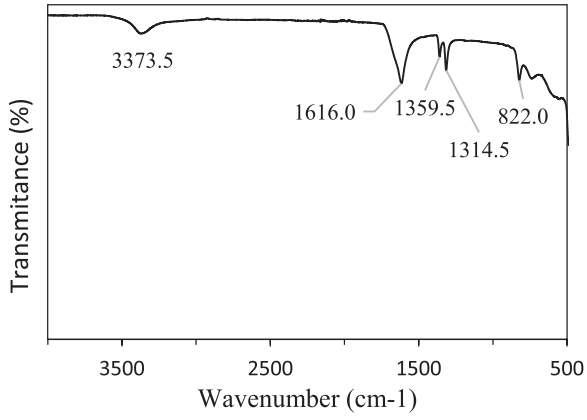

Fig. 9. FT-IR analysis of the leaching residue.

$$4H_2C_2O_4 + 2LiCo_{0.33}Ni_{0.33}Mn_{0.33}O_2 = Li_2C_2O_4 + 0.66\,CoC_2O_{4\,solid} + 0.66NiC_2O_{4\,solid} + 0.66MnC_2O_{4\,solid} + 4H_2O + 2CO_{2\,gas} \quad (15)$$

$$7H_2C_2O_4 + 2LiCo_{0.33}Ni_{0.33}Mn_{0.33}O_2 = 2LiHC_2O_4 + 0.66\,CoC_2O_{4\,solid} + 0.66NiC_2O_{4\,solid} + 0.66MnC_2O_{4\,solid} + 4H_2O + 2CO_{2\,gas} \quad (16)$$

This is in accordance with the reaction given by Bingyu Shen et al. [23], who studied the dissolution of the lithium cobalt oxide cathode material (Equations (3) and (4). The detailed mechanism still needs to be investigated to understand the different reactions occurring from the dissolution of the lithium metal oxides to their complexation with the oxalate ions. Particularly, for the dissolution of aluminum. Bingyu Shen et al. [23] proposed a dissolution of the aluminum involving a reduction of the aluminum foil (production of hydrogen) and its complexation, as seen in Equation 7. However, the aluminum complex expressed in their work, $Al(HC_2O_4)_3$, is reported insoluble, while a complete dissolution of the aluminum was observed in this study. In fact, aluminum ions can complex with the oxalate in various manners, resulting in soluble aluminum oxalate complexes, that have not been identified yet.

5. Conclusions

A very efficient way to achieve an early selective lithium recovery from spent lithium-ion batteries was demonstrated in this work. Oxalic acid, the strongest of the organic acids, reacts with lithium, nickel, manganese, and cobalt oxide to form their respective oxalates. Given the fact that lithium simple oxalate and aluminum complex oxalates are the only ones soluble, they can be selectively dissolved in the leachate using oxalic acid under optimized conditions, while the other transition metals remain in the leaching residue.

A design of experiments was performed to identify the interaction between the different leaching parameters and to identify the optimum conditions. The regression models representing the leaching yield of lithium, aluminum, copper, cobalt, manganese, and nickel were validated and contour plots helped to analyze the dissolution process. The main outcomes of this work are the following:

1) A minimum of 0.45 M of oxalic acid was required to reach a lithium dissolution of over 90%.
2) Aluminum is entirely leached under most of the tested conditions, which is a novel finding of this study since this behavior has never been reported by other authors as being that complete. It is very important to know this while developing a recycling process. The purification of the leachate solution will be done in further studies.
3) High leaching selectivity was achieved for lithium versus the other metals, which presented very low dissolution. From the transition metals, manganese was the one the more extracted with only 2.4% leaching yield in the central point of the design.

The main objective of this study was to achieve a very selective leaching operation toward lithium. The optimum parameters identified in this work are 60 °C, 60 min, and 0.6 M of oxalic acid at the fixed S/L ratio of 50 g/L. An upscaled test was performed under optimum parameters to validate the responses obtained by the models and to further investigate the leaching behavior. This allowed a very interesting appreciation of the selectivity of the operation: 98.8% of the lithium and 100% aluminum were leached, while less than 0.5 % of cobalt and nickel, and 1.5% of manganese were dissolved. The leaching rates were confirmed after analyzing the leaching residue. FT-IR proved the presence of the carboxyl group in the residue, while the presence of cobalt, manganese, and nickel oxalates formed and precipitated during the leaching was confirmed by XRD. No traces of NMC cathode active material were detected in the leaching residue. The complete leaching of aluminum consists of an essential finding for the development of this

operation in a recycling process and the purification of the leachate, which will be further investigated in future studies.

CRediT authorship contribution statement

Léa M.J. Rouquette: Conceptualization, Methodology, Investigation, Writing – original draft. **Martina Petranikova:** Supervision, Writing – review & editing. **Nathália Vieceli:** Supervision, Conceptualization, Methodology, Writing – review & editing.

Declaration of Competing Interest

The authors declare that they have no known competing financial interests or personal relationships that could have appeared to influence the work reported in this paper.

Data availability

Data will be made available on request.

Acknowledgments

This research was supported by the Swedish Energy Agency – Battery fund (Grants No: 52009-1) and BASE (Batteries Sweden) by Vinnova (Grant No. 2019-00064). The authors would like to acknowledge the support of Volvo Cars AB. Stena Recycling International AB, and Akkuser Oy for providing samples and for valuable discussions.

Appendix A. Supplementary material

Supplementary data to this article can be found online at https://doi.org/10.1016/j.seppur.2023.124143.

References

[1] Energy Agency, I. Global EV Outlook 2022 Securing Supplies for an Electric Future. **2022**.
[2] IEA, P. Electric Vehicles - Technology Deep Drive - Tracking Report Available online: https://www.iea.org/reports/electric-vehicles, License: CC BY 4.0 (accessed on 19 January 2023).
[3] European parliament Deal Confirms Zero-Emissions Target for New Cars and Vans in 2035 Available online: https://www.europarl.europa.eu/news/en/press-room/20221024IPR45734/deal-confirms-zero-emissions-target-for-new-cars-and-vans-in-2035 (accessed on 19 January 2023).
[4] U.S Geological Survey Lithium Data - Mineral Commodity Summary. *U.S Geological Survey* **2022**, 2021–2022.
[5] European Comission RMIS - Raw Materials Profile - Lithium Available online: https://rmis.jrc.ec.europa.eu/apps/rmp2/#/Lithium (accessed on 27 January 2023).
[6] European Comission RMIS – Raw Materials Profiles - Lithium Available online: https://rmis.jrc.ec.europa.eu/apps/rmp2/#/Lithium (accessed on 20 February 2023).
[7] Hampel, C. *Electrive.com*. 2022.
[8] MAISCH, M. *PV magazine*. 2019.
[9] European commission *REGULATION OF THE EUROPEAN PARLIAMENT AND OF THE COUNCIL Concerning Batteries and Waste Batteries*; 2020; Vol. 353.
[10] B. Makuza, Q. Tian, X. Guo, D.Y. Kinnor Chattopadhyay, Pyrometallurgical options for recycling spent lithium-ion batteries_ a comprehensive review, Power sources (2021) 491.
[11] J. Neumann, M. Petranikova, M. Meeus, J.D. Gamarra, R. Younesi, M. Winter, S. Nowak, Recycling of lithium-ion batteries—current state of the art, circular economy, and next generation recycling, Adv. Energy Mater. (2022), 2102917, https://doi.org/10.1002/aenm.202102917.
[12] B. Swain, Recovery and recycling of lithium: a review, Sep. Purif. Technol. 172 (2017) 388–403, https://doi.org/10.1016/j.seppur.2016.08.031.
[13] E. Gerold, C. Schinnerl, H. Antrekowitsch, Critical evaluation of the potential of organic acids for the environmentally friendly recycling of spent lithium-ion batteries, Recycling 7 (2022) 4.
[14] R. Golmohammadzadeh, F. Faraji, F. Rashchi, Recovery of lithium and cobalt from spent lithium ion batteries (LIBs) using organic acids as leaching reagents : a Review, Resour. Conserv. Recycl. 136 (2018) 418–435, https://doi.org/10.1016/j.resconrec.2018.04.024.
[15] Y. Wang, Z. Xu, X. Zhang, E. Yang, Y. Tu, A green process to recover valuable metals from the spent ternary lithium-ion batteries, Sep. Purif. Technol. 299 (2022), 121782, https://doi.org/10.1016/j.seppur.2022.121782.
[16] L. Li, J. Ge, F. Wu, R. Chen, S. Chen, B. Wu, Recovery of cobalt and lithium from spent lithium ion batteries using organic citric acid as leachant, J. Hazard. Mater. 176 (2010) 288–293, https://doi.org/10.1016/j.jhazmat.2009.11.026.
[17] X. Chen, D. Kang, L. Cao, J. Li, T. Zhou, H. Ma, Separation and recovery of valuable metals from spent lithium ion batteries: simultaneous recovery of Li and Co in a Single Step, Sep. Purif. Technol. 210 (2019) 690–697, https://doi.org/10.1016/j.seppur.2018.08.072.
[18] Krishnamurty, K. v.; Harris, G.M.; Sastri, V.S. *The Chemistry of the Metal Carbonato Complexes*; 1960; Vol. 70.
[19] B. Pospiech, M. Warzecha, Application of oxalic acid as an efficient leaching agent of aluminum from industrial waste, Physicochemical Problems of Mineral Processing 56 (2020) 264–270, https://doi.org/10.37190/ppmp19103.
[20] R. Karbouj, Aluminium leaching using chelating agents as compositions of food, Food Chem. Toxicol. 45 (2007) 1688–1693, https://doi.org/10.1016/j.fct.2007.03.001.
[21] David R. Lide *CRC Handbook in Chemistry and Physics*; Standard R.
[22] J.S. Sohn, S.M. Shin, D.H. Yang, S.K. Kim, C.K. Lee, Comparison of two acidic leaching processes for selecting the effective recycle process of spent lithium ion battery, Geosystem Eng. 9 (2006) 1–6, https://doi.org/10.1080/12269328.2006.10541246.
[23] X. Zeng, J. Li, B. Shen, Novel approach to recover cobalt and lithium from spent lithium-ion battery using oxalic acid, J. Hazard. Mater. 295 (2015) 112–118, https://doi.org/10.1016/j.jhazmat.2015.02.064.
[24] A. Verma, A.J. Henne, D.R. Corbin, M.B. Shiflett, Lithium and cobalt recovery from LiCoO2using oxalate chemistry: scale-up and techno-economic analysis, Ind. Eng. Chem. Res. 61 (2022) 5285–5294, https://doi.org/10.1021/acs.iecr.1c04876.
[25] A. Verma, G.H. Johnson, D.R. Corbin, M.B. Shiflett, Separation of lithium and cobalt from LiCoO2: a unique critical metals recovery process utilizing oxalate chemistry, ACS Sustain. Chem. Eng. 8 (2020) 6100–6108, https://doi.org/10.1021/acssuschemeng.0c01128.
[26] A. Verma, D.R. Corbin, M.B. Shiflett, Lithium and cobalt recovery for lithium-ion battery recycle using an improved oxalate process with hydrogen peroxide, Hydrometall 203 (2021), 105694, https://doi.org/10.1016/j.hydromet.2021.105694.
[27] Q. Li, K.Y. Fung, L. Xu, C. Wibowo, K.M. Ng, Process synthesis: selective recovery of lithium from lithium-ion battery cathode materials, Ind. Eng. Chem. Res. 58 (2019) 3118–3130, https://doi.org/10.1021/acs.iecr.8b04899.
[28] L. Sun, K. Qiu, Organic oxalate as leachant and precipitant for the recovery of valuable metals from spent lithium-ion batteries, Waste Manag. 32 (2012) 1575–1582, https://doi.org/10.1016/j.wasman.2012.03.027.
[29] X. Zhang, Y. Bian, S. Xu, E. Fan, Q. Xue, Y. Guan, F. Wu, L. Li, R. Chen, Innovative application of acid leaching to regenerate Li(Ni1/3Co1/3Mn1/3)O2 cathodes from spent lithium-ion batteries, ACS Sustain. Chem. Eng. 6 (2018) 5959–5968, https://doi.org/10.1021/acssuschemeng.7b04373.
[30] Retsch *An Expert Guide to Particle Size Analysis*; 2015.
[31] R.W. Gerlach, D.E. Dobb, G.A. Raab, J.M. Nocerino, Gy sampling theory in environmental studies. 1. assessing soil splitting protocols, J. Chemom. 16 (2002) 321–328, https://doi.org/10.1002/cem.705.
[32] Douglas C. Montgomery *Design and Analysis of Experiments*; John Wiley & Sons, Ed.; 2009; ISBN 978-0-470-39882-1.